

Target Detection and Recognition in SAR Imagery Based on KFDA

Fei Gao¹, Jingyuan Mei^{1,}, Jinping Sun¹, Jun Wang¹, Erfu Yang², Amir Hussain³*

1. School of Electronic and Information Engineering, Beihang University, Beijing 100191, China

2. Space Mechatronic Systems Technology Laboratory (SMeSTech), Department of Design, Manufacture and Engineering Management, University of Strathclyde, Glasgow G1 1XJ, UK

3. Cognitive Signal-Image and Control Processing Research (COSIPRA) Laboratory, School of Natural Sciences, University of Stirling, Stirling FK9 4LA, UK

Abstract---Current research on target detection and recognition from synthetic aperture radar (SAR) images is usually carried out separately. It is difficult to verify the ability of a target recognition algorithm for adapting to changes in the environment. To realize the whole process of SAR automatic target recognition (ATR), especially for the detection and recognition of vehicles, an algorithm based on kernel fisher discriminant analysis (KFDA) is proposed in this paper. First, in order to make a better description of the difference between background and target, KFDA is extended to the detection part. Image samples are obtained with a dual-window approach and features of the inner and outer window samples are extracted using KFDA. The difference between the features of inner and outer window samples is compared with a threshold to determine whether a vehicle exists. Second, for the target area, we propose an improved KFDA-IMED (Image Euclidean Distance) combined with a support vector machine (SVM) to recognize the vehicles. Experimental results validate the performance

of our method. On the detection task, our proposed method obtains not only a high detection rate but also a low false alarm rate without using any prior information. For the recognition task, our method overcomes the SAR image aspect angle sensitivity, reduces the requirements for image preprocessing and improves the recognition rate.

Keywords: synthetic aperture radar; target detection; kernel fisher discriminant analysis; target recognition; image Euclidean distance; support vector machine

1. Introduction

Synthetic aperture radar (SAR) extends the radar signal to two dimensions and greatly enriches the information acquired. It has become a landmark in the history of development of radar technology.

With the increase of radar coverage area and continuous development in SAR imaging technology, the amount of SAR images has far exceeded the limit of current image interpretation capability. The development of SAR sensors is moving to high-resolution, multi-mode, multi-frequency,

multi-polarization and multi-band, which makes the information in SAR images more abundant but also demands higher requirements for target detection and recognition. Thus SAR ATR (automatic target recognition) has become one of the hottest topics in the field of military defense over the past 20 years. In particular, vehicle (such as armored vehicle, tank, car, etc.) detection and recognition are two important branches of SAR ATR. Researchers have thus proposed a variety of effective algorithms for these two emerging areas.

There are two categories of algorithms for vehicle detection in SAR images. The first is based on the contrast of pixels such as constant false alarm rate (CFAR) which is the most classic and the most widely used algorithm. Novak et al. [1] derived a highly influential two-parameter CFAR detector with an assumption that the amplitude distribution of the clutter is Gaussian, which opened a new chapter for target detection in SAR images. The development of many derivative algorithms such as OS-CFAR, VI-CFAR and EF-CFAR has since followed. However, in the current situation, CFAR also faces enormous challenges. The main problem is that CFAR always yields a high false alarm rate under a complex environment and weak-target condition as a result of ignoring the target's own features. The detection result also strongly depends on the selected distribution model while there are considerable difficulties in building a universal distribution model. The

second category is based on a number of other features of SAR images. Researchers in [2, 3] introduced the concept of knowledge and proposed a detection method based on prior knowledge and context information respectively. These algorithms can fully use the prior information although much of it is often hard to obtain for strange geographical environments. Researchers in [4] developed a multi-resolution algorithm for detecting man-made objects in SAR images. Authors in [5] used shadow information as a prescreening feature to improve detection performance. One of the disadvantages for works reported in [4, 5] is that they apply complex advanced features such as multi-resolution and shadow. The access to these advanced features is not easy and also a large amount of calculation is needed. Recently, a novel vehicle detection algorithm based on the visual attention mechanism [6] has become a major research focus and is attracting growing attention of researchers.

There are also two categories of vehicle recognition algorithms in SAR images. The first is model-based algorithm. In the literature [7-9] B. Bhanu et al. described their contribution to model building. They predicted a series of associated candidate targets through the mathematical models and made a judgment by matching. The disadvantage of such algorithms is that building an SAR image model a high level of theoretical basis and calculation is needed. The second category is that of template-based algorithms. Previous

researchers [10] proposed a typical method using original SAR images or sub-images as templates. However, this method is extremely sensitive to changes in depression angle and aspect angle so that it requires a large number of templates. In recent years with the rapid development of feature extraction algorithms and classification algorithms, many feature-based classification algorithms for SAR images are proposed. For feature extraction algorithms, works reported in [11, 12] characterized the features of scattering centers and used Prony model and Attributed model respectively. The work of [13] demonstrated the feasibility of recognizing vehicle targets in SAR images using the peak feature. Work in [14] presented twenty features (namely the standard deviation feature, fractal dimension feature etc.) as an evolutionary feature synthesis. The selection of these features is a difficult task. If we select only one feature, this reflects the unilateral information of the targets, which may cause large deviation with a small number of training samples. If some of the features are combined as feature synthesis, different synthesis lead to different recognition results since each feature may not be valid in a certain condition. Complexity can be increased by using more features, yet it does not necessarily mean a better result. However, this difficult task gives rise to various linear or nonlinear transformation algorithms, which are another important branch of feature extraction algorithms. These transformation

algorithms try to extract global features from the entire image, which can remove redundant information and achieve dimensionality reduction. Linear principle component analysis (PCA) is applied in [15] to extract features. The disadvantage of PCA is that it only considers second-order correlation between the samples and ignores the higher order statistics. In other works [16], classic nonlinear kernel principal component analysis (KPCA) is used but simulation results show that the ability of KPCA to extract discriminative features is not effective. In recent years, the idea of manifold ways of perception [17] has also been introduced to the field of SAR image feature extraction and become a popular research focus. For classification algorithms following the feature extraction stage, researchers in [18, 19] used support vector machine (SVM) for SAR vehicle recognition and set off a new wave of research. Adaboost is also used in [20], which has also been widely promoted. Currently SVM and Adaboost have demonstrated a lot better performance compared other algorithms.

A vehicle is often presented as a substantially rectangular bright spot in SAR images. With the improvement of camouflage technology, strong scatters of the vehicle are reduced so that target pixels and background pixels have less difference. When the vehicle is planning to escape detection and remains adjacent to other structures in the complicated environment, key pixels are consequently

decreasing and interference pixels increasing. Some important features like scattering centers, object outline and shadow information are destroyed, so that traditional detection algorithms based on contrast such as CFAR and others based on feature synthesis do not deliver the required performance.

In this paper, we attempt to use the global features difference between the vehicle and surrounding environment to improve the detection performance of hidden targets. As kernel methods have been successfully applied to classification, we hope kernel methods can be introduced into detection in SAR images, which is essentially a classification problem between two classes. KFDA is a well-known discriminative feature extraction criterion of pattern class. It looks for a projection direction in a high-dimensional space, which can make the samples of different classes separated as far as possible with samples in the same class gathered as close as possible. Thus, after acquiring the target samples and clutter samples with a dual-window approach, the use of KFDA to calculate the difference between the two classes to achieve target detection may exhibit certain advantages. Simulation results show that application of the KFDA to SAR vehicle detection demonstrates performance. It considers target features so that it can reduce false alarms which are highly bright and similar to the targets in traditional target detection algorithms [1]. Furthermore, without the use of prior information, as in literature [2, 3], our KFDA method also avoids the

difficulty of selecting and extracting advanced features [4, 5] and obtains a high detection rate and low false alarm rate. For SAR target recognition, the differences between each class of vehicle are subtle and highly localized in few pixels. And for the case of real-world conditions, vehicles include variations in aspect angle, target configurations and obscuration due to occlusion and layover. These difficulties place great burden on algorithms using one feature or a feature synthesis. In this paper, we attempt to exploit the efficiency of KFDA for extracting global nonlinear features of SAR vehicle in order to improve the recognition rate. In order to clearly reflect the spatial relationship and the deformation degree between two images, IMED is embedded in KFDA as an improved KFDA-IMED. Simulation results demonstrate that our KFDA-IMED method produces good recognition results for both the exposed targets and hidden targets and avoids the difficulties of selecting features as in literature [11-14] without pre-processing and image segmentation.

This paper proposes an organically integrated vehicle detection and recognition algorithm for SAR images based on KFDA. If training samples are not available, detection can still be achieved. Or if training samples are available, it can also enable vehicle recognition and validate the detection results in auxiliary. Furthermore, clutter samples can be collected from some of the background regions in the recognition part in order to

reduce the number of false alarms generated in the detection part.

This paper is structured as follows. Section 2 presents KFDA (KFDA-IMED). The proposed SAR vehicle detection and recognition algorithm based on KFDA is described in Section 3. In Section 4, the experimental results of SAR vehicle detection and recognition are presented. We also analyze the adaptability of the recognition algorithm to the diversity of the environment clutter and the influence of size of target image chip on the recognition rate. Section 5 presents some concluding remarks.

2. KFDA and Improved

KFDA-IMED

Assuming two different classes of n dimensional input samples can be projected to a higher dimensional feature space F by a nonlinear mapping $\phi: x \in R^n \rightarrow \phi(x) \in F$, better linear separability of the samples can be obtained in the higher dimensional feature space. Following this their features can be extracted through the well-known Fisher's LDA (FLDA) [21].

Let X denote an input sample set comprising N samples; X_i denote a subset of X comprising N_i samples; and $c(c \leq n)$ denote the number of classes, thus

we have, $X = \bigcup_{i=1}^c X_i$, $N = \sum_{i=1}^c N_i$. The

input samples $x_j^i \in X_i$ and $x_j \in X$ can be mapped respectively in the higher dimensional feature space F as $\phi(x_j^i) = \phi_j^i$ and $\phi(x_j) = \phi_j$. The within-class scatter matrix of samples in the space F is defined by:

$$S_w^\Phi = \frac{1}{N} \sum_{i=1}^c \sum_{j=1}^{N_i} (\phi_j^i - m_i^\Phi)(\phi_j^i - m_i^\Phi)^T \quad (1)$$

where $m_i^\Phi (m_i^\Phi = \frac{1}{N_i} \sum_{j=1}^{N_i} \phi_j^i)$ is the mean of each class of samples in the space F and S_w^Φ characterizes the degree of aggregation of internal samples in each class. While the between-class scatter matrix of samples in the space F is defined by:

$$S_b^\Phi = \frac{1}{N} \sum_{i=1}^c N_i (m_i^\Phi - m_0^\Phi)(m_i^\Phi - m_0^\Phi)^T \quad (2)$$

where $m_0^\Phi (m_0^\Phi = \frac{1}{N} \sum_{j=1}^N \phi_j = \frac{1}{N} \sum_{i=1}^c N_i m_i^\Phi)$ is the mean of all the samples in the space F and S_b^Φ characterizes the degree of dispersion among the different classes.

In the space F , FLDA looks for the projection direction w to make the samples of different classes separated as far as possible, whilst and the samples in the same class are gathered as close as possible. This goal can be written as:

$$\max_w J^\Phi(w) = \frac{w^T S_b^\Phi w}{w^T S_w^\Phi w} \quad (3)$$

(3) is termed the so-called Rayleigh quotient [22].

The derivation above is the Fisher's criterion in the high-dimensional feature space. In order to derive KFDA, based on reproducing kernel theory, w can be expanded as:

$$w = \sum_{j=1}^N \alpha_j \phi_j \quad (4)$$

where α_j is the coefficient. With (4), (3) can be changed to

$$\max_a J(\alpha) = \frac{\alpha^T K_b \alpha}{\alpha^T K_w \alpha} \quad (5)$$

where $\alpha = [\alpha_1, \alpha_2, \dots, \alpha_N]^T$ is the KFDA vector in the space F ;

$K_w = \frac{1}{N} \sum_{i=1}^c K_i (I - \frac{1}{N_i}) K_i^T$, where I is

an $N_i \times N_i$ identity matrix, $\frac{1}{N_i}$ is an

$N_i \times N_i$ matrix with each entry equal to

$\frac{1}{N_i}$, $K_i = [k(x_j, x_j^i)]$ is an $N \times N_i$

matrix with the introduced kernel function $k(\bullet, \bullet)$ [23];

$K_b = \frac{1}{N} \sum_{i=1}^c N_i (G_i - G_0)(G_i - G_0)^T$, where

$G_i = \left(\frac{1}{N_i} \sum_{j=1}^{N_i} k(x_1, x_j^i), \dots, \frac{1}{N_i} \sum_{j=1}^{N_i} k(x_N, x_j^i) \right)^T$,

$G_0 = \left(\frac{1}{N} \sum_{j=1}^N k(x_1, x_j), \dots, \frac{1}{N} \sum_{j=1}^N k(x_N, x_j) \right)^T$. If

Lagrange multipliers are introduced, the calculation of α can be solved simply by finding the $c-1$ most significant eigenvectors of $K_w^{-1} K_b$ in the following form:

$$\lambda \alpha = K_w^{-1} K_b \alpha \quad (6)$$

For every input sample x , the features extracted by KFDA is actually the projection of $\phi(x)$ in the optimal direction w . Thus, each dimensional element of the features is

$$z_i = w_i \bullet \phi(x) = \sum_{j=1}^N \alpha_j^i k(x_j, x) \quad (7)$$

where α_j^i is the j th element of the i th significant eigenvector of $K_w^{-1} K_b$. The

feature, which is extracted by KFDA,

$z = [z_1, z_2, \dots, z_{c-1}]^T$ is an $c-1$

-dimensional vector. Compared with the whole image, KFDA reduces the dimensions significantly. The derivation in this section shows that the nonlinear feature extraction criterion KFDA actually calculates the Fisher discriminant in the high-dimensional feature space using the kernel method.

When the radial basis function (RBF)

$k(x, y) = \exp(-\frac{\|x-y\|^2}{2\sigma^2})$ is selected as the

kernel function $k(x, y)$, as x and y are two images not common vectors in target recognition, it only calculates the traditional Euclidean distance between them and ignores

the spatial relationships among the pixels so it is extremely sensitive even to small deformations. To tackle this disadvantage, we embed IMED in KFDA [24]. IMED can reflect the correlation among the image samples better since it is invariant to the linear transformation of the images, and depends on the extent of the deformation.

Let $P_1 = (P_1^1, P_1^2, \dots, P_1^n)$ and $P_2 = (P_2^1, P_2^2, \dots, P_2^n)$ denote two H by L images, where $H \times L = n$. The element $g_{ij}(i, j = 1, 2, \dots, n)$ of the image metric matrix $G_{n \times n}$ reflects the relationship of position between pixel P^i and pixel P^j . Assuming the location of P^i is (h, l) and the location of P^j is (h', l') , g_{ij} can be written as:

$$g_{ij} = \frac{1}{2\pi} \exp\{-|P^i - P^j|^2 / 2\} \quad (8)$$

where $|P^i - P^j| = \sqrt{(k - k')^2 + (l - l')^2}$.

Thus, IMED between P_1 and P_2 is:

$$\begin{aligned} IMED &= \frac{1}{2\pi} \sum_{i,j=1}^n \exp\{-|P^i - P^j|^2 / 2\} \\ &= (P_1^i - P_2^j)(P_1^j - P_2^i) = \\ &= (P_1 - P_2)^T G (P_1 - P_2) \end{aligned} \quad (9)$$

Then the calculation of RBF with IMED is:

$$\begin{aligned} k(P_1, P_2) &= \\ \exp\left[\frac{-1}{2\sigma^2} (P_1 - P_2)^T G (P_1 - P_2)\right] &= \\ \exp\left(\frac{-1}{2\sigma^2} IMED\right) \end{aligned} \quad (10)$$

For large images, the evaluation of G is expensive. The standardizing transform (ST) [24] or Kronecker product [25] can be introduced to simplify the calculations.

In the above derivation, the process of calculating Rayleigh quotient and extracting the features were based on the assumption that the within-class scatter matrix K_w is a nonsingular matrix. However, according to Fisher's criterion, K_w is a nonsingular matrix only if the number of training samples is greater than the dimension of sample space. Otherwise K_w is a singular matrix and thus the inverse does not exist. To avoid such ill-conditioned settings, K_w can be replaced by $K_w \approx K_w + \kappa I$. Here I is an identity matrix of the same order of K_w , and the constant κ which acts as a disturbance, is small and greater than zero. The properties of $K_w \approx K_w + \kappa I$ will be dominated by κ if κ is too large, which means the degree of aggregation of the internal samples in each class is restricted. This will make the feature eigenvector α disturbed, and the features of each class relatively dispersed, and the recognition rate gets reduced. κ is often set to be $\kappa \leq 10^{-3}$.

KFDA and improved KFDA-IMED above constitute the core theory of proposed algorithms in this paper. Their flow chart is shown in Fig. 1.

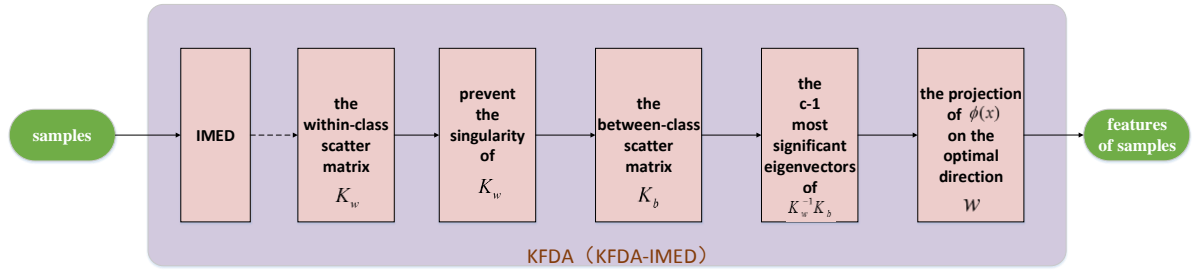


Fig. 1 Flow-chart of KFDA and improved KFDA-IMED

3. Algorithm Description

3.1 Vehicle Detection

The SAR vehicle detection algorithm proposed in this paper introduces KFDA to extract the discriminative features of the vehicle and its surrounding environment and calculates the difference between features to determine its existence. An edge preserving smoothing operation and grey scale quantization [2] are performed on the original SAR image in order to reduce the impact of speckle noise while preserving the boundary edges of a vehicle.

In general, a target has stronger scattering properties than its surrounding area while the target pixels are only a tiny part of the whole SAR image. Therefore we can choose an appropriate global threshold to achieve image binarization and determine possible target pixels so we do not need to carry out traversal search for the overall image. When the vehicle stays adjacent to trees for hiding, another

advantage for the global threshold operation is that it can separate the pixels of trees and the pixels of vehicles. For the case of trees, there are many gaps between leaves, and part of the electromagnetic waves will be reflected directly by trees while some will be reflected by the ground. From Fig. 2 we can see that trees show a mixture of bright spots and dark spots. Fig. 3 shows the results of performing the edge preserving smoothing operation, grey scale quantization and the global threshold operation. It is obvious that the trees are separated into discrete points by the global threshold so that it is conducive to detect vehicles around the trees. However in Fig. 3, some bright spots can still be found, which are similar to the vehicles and produced by trees. False alarms may be caused by these bright spots. In subsequent processing, we will try to eliminate these kinds of bright spots through the extraction of appropriate features of KFDA.

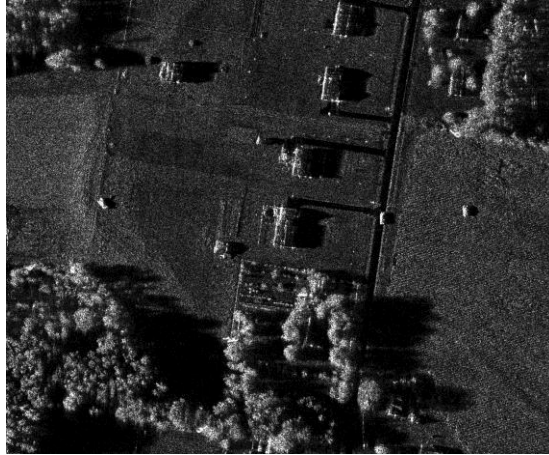


Fig. 2 original SAR image



Fig. 3 SAR image after the global threshold operation

After the global threshold operation, two obvious problems still confront us. First, there are still a great number of discrete non-target points in the image. Second, some dark points of the vehicles are excluded. Morphological filtering can be used to eliminate those discrete and small points and make the target region more homogeneous, whilst preserving its edge information [26].

All the left bright spots in the binary image can belong to the vehicles, which need to be examined one by one. Before this, we perform image segmentation with connected component analysis, wherein each bright spot is assigned an index number and the

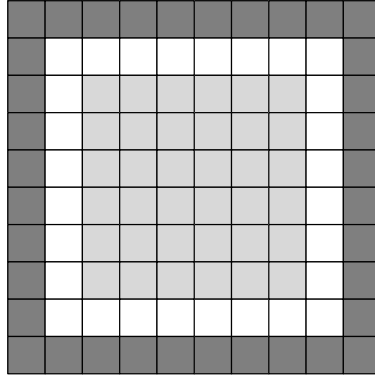
coordinate of each bright spot pixel is recorded. This way, traversing all the pixels in the subsequent detection process is not needed.

Until now, the number of bright spots in the binary image may still be large. While some obvious non-target spots can be simply excluded on the basis of their size or shape. For example, a long and thin bright spot can be ignored directly because its shape does not match the shape of a vehicle.

Next, the KFDA is operated with the dual-window approach, which is the core steps of our proposed detection algorithm. The size and shape of the inner-window is determined according to the general size and

shape of vehicles. The shape of the protecting window and the outer-window is the same as the inner-window. The protecting window is slightly larger than the inner-window whilst still smaller than the outer-window. Finally, the number of pixels in the outer-window is the same as in the inner-window. The

dual-window approach used in this paper is shown in Fig. 4. The center of the dual-window can be located in each bright spot's geometric center, which is calculated with the coordinates of pixels of each bright spot in the original SAR image, using the index number.



□ inner-window □ protecting window ■ outer-window

Fig. 4 The form of dual-window

In detection, we make the current inner-window move to different directions in the protecting window to get a series of inner-window samples, which are termed the inner-window sample set. Meanwhile, the current outer-window is moved to the same directions as the inner-window to get a series of outer-window samples termed the outer-window sample set. Since the outer-window has a certain width, some part of the target pixels may also be covered. Therefore, we set the number of leaked pixels to be D , which means that the D brightest pixels in each outer-window sample and the D darkest pixels in each inner-window sample will be eliminated. The value of D can be determined based on the width of the

outer-window.

The complex diversity of the SAR image makes it necessary to normalize the amplitude of each inner-window sample and each outer-window sample. The normalization formula is given by:

$$\mathbf{x}_{Normalized} = \frac{\mathbf{x}}{\|\mathbf{x}\|_2} \quad (11)$$

where \mathbf{x} is the vector representation of each sample; and $\mathbf{x}_{Normalized}$ the vector representation of the normalized \mathbf{x} .

Let X_1 denote the normalized inner-window sample set and X_2 the normalized outer-window sample set. The feature of current inner-window sample z_i

and the feature of current outer-window sample z_o are extracted with KFDA through equations (1-7). Both z_i and z_o are one dimensional. The detection is achieved by comparing the difference between z_i and z_o with a threshold as follows:

$$z_i - z_o \begin{matrix} > T \\ < T \end{matrix} \begin{matrix} H_1 \\ H_0 \end{matrix} \quad (12)$$

where H_1 implies that the current

inner-window sample is a vehicle; H_0 implies the current inner-window sample is clutter; and T is the threshold.

The above SAR vehicle detection algorithm based on KFDA is outlined in the upper half of Fig. 5, which shows that the detection result can be output directly. The lower half of Fig. 5 also shows our proposed recognition algorithm based on the KFDA-IMED when training samples are available.

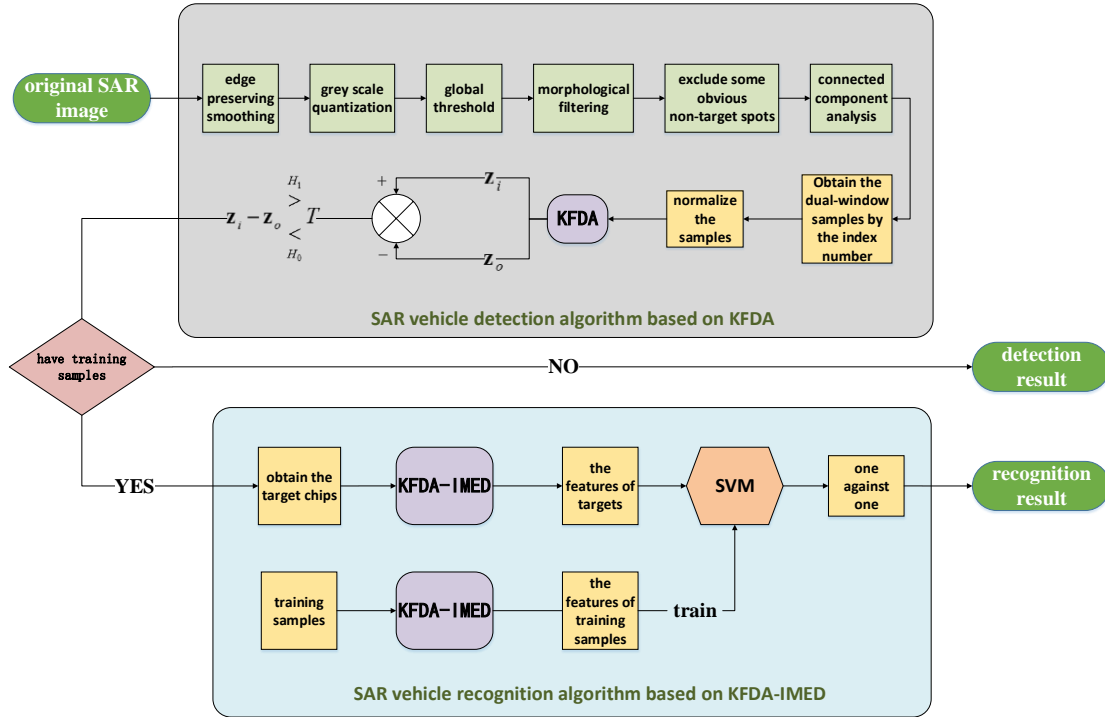


Fig. 5 Flow-chart of SAR vehicle detection and recognition algorithm based on KFDA

3.2 Vehicle Recognition

After the detection stage, the types of H_1 image samples can be recognized if we

have the same types of vehicles in our training sample database. In this case, firstly, the H_1 image chips are collected from the original SAR image. Second, the amplitude of each training sample and each H_1 image chip

should be normalized with (11). Third, the features of training samples and H_1 image chips are extracted with the KFDA-IMED through (1-10). The features of each training sample or each H_1 image chip can be represented as a $c - 1$ dimensional vector.

In this paper, the well-known SVM is chosen for features classification. The reasons are two-fold: firstly, SVM is based on the structural risk minimization basis so ensures theoretical generalization; secondly, the SVM has advantages in solving small sample size and nonlinear problems and is relatively insensitive to the representation of features. SVM is trained with the features of training samples. The recognition of H_1 image chips is executed according to the “one-against-one” multiclass strategy.

In the following step, we address a problem when false alarms in the detection may be incorrectly recognized as one type of vehicle. For this case, some environmental samples can be collected before recognition in certain areas which are around yet do not cover the H_1 image chips. We hope this approach can make the false alarms recognizable as environment samples and thus be removed. However, this operation also raises another problem. If the undetected targets are collected as environment samples, the credibility of the recognition results is seriously affected. Hence, it is necessary to set the threshold T lower to guarantee the

absence or the presence of only few undetected targets before the environment samples collection step.

In much of the literature [15, 16, 26, 27], researchers have performed some pre-processing operations for enhancing recognition, such as log transformation, Fourier transform, image segmentation, power-law transformation, image filtering and so on, and consequently obtained a high recognition rate. In this paper, however, after obtaining H_1 image chips from the original SAR image, only the simple normalization operation is applied. The main reasons can be summarized as follows: first, we believe the KFDA-IMED demonstrates a consistently high efficiency in terms of feature extraction and can reduce the requirements for image preprocessing; second, these complex pre-processing operations do not lead to a definitively higher recognition rate for our KFDA-IMED. Specifically, our experience has shown that not every pre-processing operation has a positive effect on the recognition rate for different feature extractions. For the case of our proposed KFDA-IMED method, the recognition rate was not found to be improved by any of the other pre-processing operations reported in the literature.

4. Experiments

4.1 Machine Learning for the Vehicle Recognition Experiment

In this experiment, spotlight SAR images of ground vehicles in the moving and stationary target acquisition and recognition (MSTAR) database [28] is used. The database provides many different types of vehicle samples which can be used for quantitatively analyzing the training process and recognition results of the algorithm proposed in this paper. The original size of SAR vehicle sample is 128×128 pixels. The resolution is $0.3m \times 0.3m$. The azimuth coverage of each type of the vehicle is $0^\circ \sim 360^\circ$ and the interval is approximately 1° . We choose three distinct types of these in the database, namely: three BMP2s (sn-c21, sn-9563, sn-9566), one BTR70 (sn-c71) and three T72s (sn-132, sn-812, sn-s7). The different serials in the same type are mainly because of the configuration variants [29], which are termed as variant targets.

The training set includes three training sample sets (BMP2sn-c21, BTR70sn-c71 and T72sn-132) at 17° depression angle. The number of samples in each training set is 232. The testing set includes all 7 serials at 15°

depression angle. BMP2sn-c21, BTR70sn-c71 and T72sn-132 are the same serial targets while BMP2sn-9563, BMP2sn-9566, T72sn-812 and T72sn-s7 are the variant targets. The number of samples in each testing set is 191.

Five recognition algorithms are compared in this experiment: SVM, KPCA+SVM, KPCA+FLDA+SVM, KFDA+SVM, KFDA-IMED+SVM. The kernel functions in KPCA and KFDA are selected as the easier-to-control polynomial function $k(x, y) = (x \bullet y + 1)^l$, where $l = 5$. The kernel function in KFDA-IMED is selected as the improved RBF

$$k(x, y) = \exp\left(-\frac{(x - y)^T G(x - y)}{2\sigma^2}\right),$$

where σ is the mean of IMED of all the training samples. The constant κ is 10^{-4} . The kernel function in SVM is selected as the RBF $k(x, y) = \exp(-0.6 \|x - y\|^2)$. The obtained recognition rates are listed in Table 1.

Table 1. Recognition rates of five different algorithms

algorithm	same serial targets	variant targets
SVM	98.08%	88.09%
KPCA+SVM	99.30%	85.86%
KPCA+FLDA+SVM	99.47%	89.92%
KFDA+SVM	99.47%	90.45%
KFDA-IMED+SVM	99.65%	91.49%

As shown in Table 1, inputting the normalized samples into SVM directly

produces good results, which demonstrates that the SVM can effectively overcome the SAR image aspect angle sensitivity problem and is suitable for SAR image processing. However, the number of normalized sample dimensions is 16384 (128×128), which contains a lot of redundant information and leads to computational complexity problems. If the KPCA is used to extract features, the number of dimensions can be effectively reduced from 16384 to 696. The KPCA approach facilitates calculations and its recognition rate of identical serial targets increases, while the rate of variant targets falls. This demonstrates that the KPCA is not efficient in extracting discriminative features of variant targets. For the case of KPCA+FLDA+SVM, the recognition rates of same serial targets and variant targets are both better than the KPCA+SVM and SVM methods. Meanwhile, the number of sample

dimensions is compressed into two, which demonstrates that the introduction of the FLDA can improve the ability to extract discriminative features. For KFDA+SVM, both rates are higher than 90%. Introducing IMED on this basis, the recognition results are further improved, which proves the effectiveness of considering the spatial relationships among pixels. The KFDA-IMED features of BMP2sn-9563 and the training set are shown in Fig. 6. The features of three training sample sets (BMP2sn-c21, BTR70sn-c71 and T72sn-132) are separated well and the features of BMP2sn-9563 are also gathered well around BMP2sn-c21. Fig. 6 demonstrates that the features can be extracted by KFDA-IMED robustly. In addition, the kernel parameters for KFDA-IMED can be calculated with the samples, which demonstrates its superior adaptability.

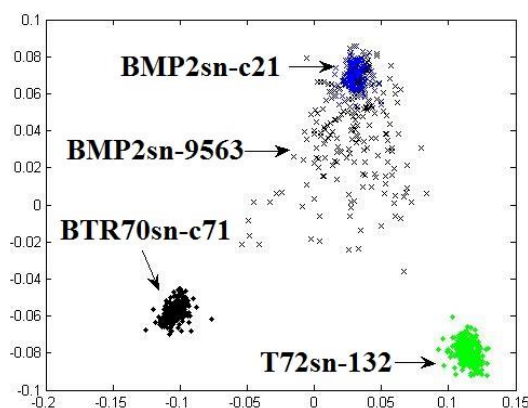


Fig. 6 The KFDA-IMED features of BMP2sn-9563 and the training set

The vehicles may appear in a range of

complicated environments. In order to demonstrate the influence of size of image chip on the recognition results, all serials of

vehicles in different sizes are recognized with the KFDA-IMED+SVM approach.

The recognition results are listed in Table 2.

Table 2. Recognition results of vehicles in different size

Size	Same Serial Targets	Variant Targets
128×128	99.65%	91.49%
112×112	99.65%	91.75%
96×96	99.83%	92.28%
80×80	100%	91.36%
64×64	100%	90.31%
48×48	100%	89.92%
32×32	100%	85.21%

It can be seen from Table 2 that, for same serial targets, reducing the size of the image chip can lead to a gradual increase in the recognition rate. For the case of variant targets, reducing the size of the image chip can make the recognition rate gradually increase at first before starting to fall. The turning point or threshold appears to be the image chip size 96 × 96. For a more detailed analysis of the experimental data, we show T72sn-812 in three different sizes (128×128, 96×96, 32×32) in Fig. 7. We can see that the pixels of both the target and the shadow are completely preserved if the image size is larger than 96×96. When the image size is smaller than 96×96, the shadow information is lost. When the image size is reduced to 32×32, a small part of the target pixels are lost as well. Fig. 7 combined with Table 2, shows that for the same serial targets, when the vehicles

themselves have no difference, only relying on the target pixels leads to good recognition results. If most of the target pixels are contained in the image chip, the size change has little effect on the recognition rate but too many background clutter pixels are likely to cause interference. When the target pixels and shadow pixels are all contained in the image chip, reducing the background clutter pixels will improve the recognition rate for the variant targets. When the shadow information is lost gradually, the recognition rate begins to decrease. Our experimental results demonstrate that important discriminative information is contained in shadow pixels, which can help recognize variant targets. Further, in order to avoid excessive interference, the irrelevant background clutter pixels need to be reduced.

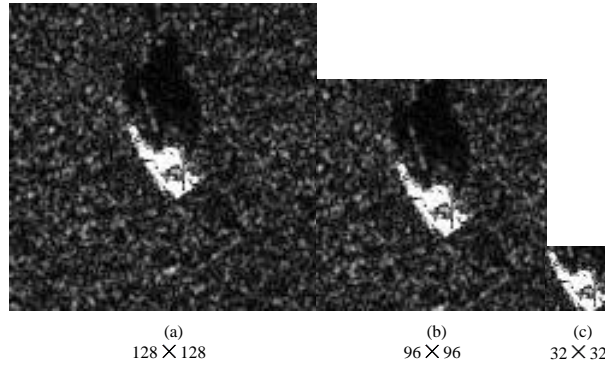


Fig. 7 T72sn-812 image chip in three different sizes

4.2 Vehicle Detection and Recognition Experiment

In this experiment, nine vehicle chips (at 15° depression angle) are inserted into a

1478×1784 full clutter MSTAR SAR image [5]. Fig. 8 shows the image with nine vehicles. White frames are used to indicate the locations of vehicles and serial numbers of the nine vehicles, one of which is seen on the road, two on grass and the other six in groves.



Fig. 8 The MSTAR SAR image with nine vehicles

Our proposed KFDA algorithm is compared with the classic CFAR algorithm for vehicle detection. In our method, the selection of the shape and size of the sliding window is mainly based on the general shape and size of vehicles. According to the analysis of Fig. 7, the size of inner-window is set at 48×48 . In order to make the number of pixels in the outer-window same as the inner-window, we

set the size of the protecting window at 55×55 and the size of the outer-window at 73×73 . As for the kernel function, we choose the easier-to-control polynomial function $k(x, y) = (x \bullet y + 1)^l$, where $l = 5$. The constant κ is 10^{-4} . The detection result is shown in Fig. 9. The nine vehicles are all detected (shown in red) and the number of false alarms is 4 (shown in white). For CFAR,

the detection result is shown in Fig. 10. Eight vehicles are detected (shown in red) and the number of false alarms is 10 (shown in white). Since CFAR mainly considers the contrast feature and ignores geometric information and features of vehicles, it is possible to generate many false alarms in a complicated environment. It is also hard to detect shaded vehicles because of the weak contrast.

However, our KFDA algorithm considers the geometric information, features of vehicles as well as the difference between features of vehicles and their surrounding environment and does not need to face the challenges of selection and extraction of the features. It has a better description and understanding of the vehicles and can produce a higher detection rate and lower false alarm rate.

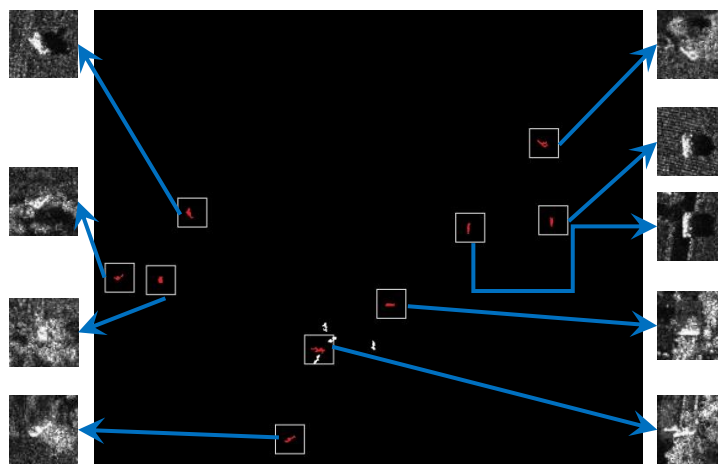


Fig. 9 Detection results of the algorithm based on KFDA (Red: vehicles. White: false alarms.)

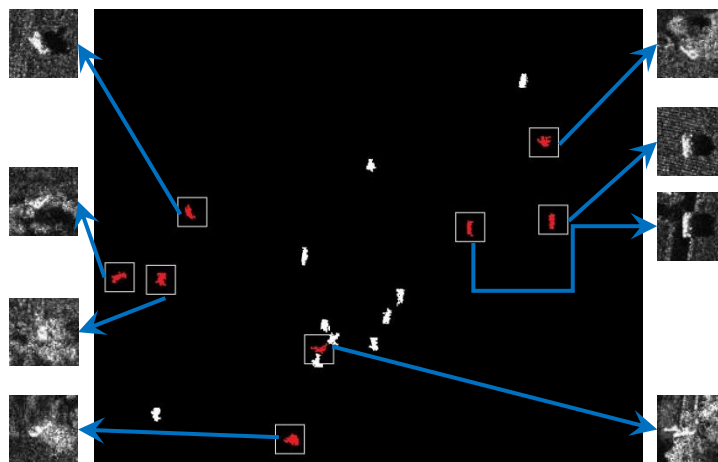


Fig. 10 Detection results of CFAR (Red: vehicles. White: false alarms.)

After detection, the geometric center of each target is locked again to collect the 48×48 image chips. The image chip of the second vehicle is shown in Fig. 11. It is obvious that a lot of pixels of trees are mixed in the image

chip. It may lead to a substantial interference with the recognition. According to the analysis of Table 2, the size of image chip is reduced to 32×32 and our KFDA-IMED approach and trained SVM in experiment 4.1 are employed to recognize the targets. The recognition

results are shown in Fig. 12 for the detected targets. ‘Red’ represents correct recognition results and ‘black’ represents wrong results. Their correct serial numbers are indicated in parentheses. 7 vehicles are correctly recognized and the recognition rate is 77.78%. For the 4 false alarms, recognition results from left to right are: BTR70, BMP2, BMP2 and BTR70. As mentioned about, some environment samples in certain areas can be

collected, which are around yet do not cover the H_1 image chips. The 4 false alarms now are recognized as background, background, BMP2 and background respectively. Meanwhile, the recognition results of the 9 vehicles remain unchanged. This process illustrates that the recognition algorithm can help eliminate 3 false alarms.



Fig. 11 48×48 image chip of the second vehicle

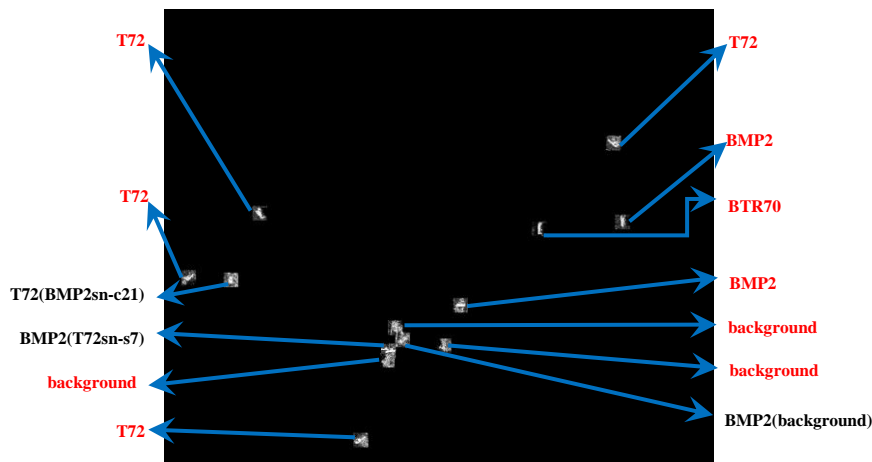


Fig. 12 Recognition results of KFDA-IMED+SVM

(‘red’ represents the correct recognition results and ‘black’ represents the wrong recognition results whose correct serial numbers are indicated in parentheses.)

There are two main reasons why the recognition rate in this experiment is lower than that in experiment 4.1. First, part of the target pixels and shadow information are lost as reducing the size of image chips, which may result in a lower recognition rate. Second, because most vehicles are in the groves, they are partially shaded by trees. This dramatically

changes and masks the pixels of vehicles and their shadows, which increases the difficulties of accurate recognition. For the 3 clearly exposed targets, the recognition results are all seen to be correct. These experimental results conform to our theoretical analysis.

5. Conclusions

Target detection and recognition are key

issues in SAR image applications. By analyzing the mathematical principles of KFDA and relevant features of vehicles, we proposed a vehicle detection method based on KFDA and a vehicle recognition method based on the improved KFDA-IMED. Experimental results with the MSTAR database demonstrate: First, our detection method does not need any prior information and avoids the difficulty of selecting features and extracting advanced features, which proves the advantages of introducing KFDA into detection. Second, our method performs better than the traditional CFAR algorithm when vehicles are shaded in a complicated environment. Third, KFDA-IMED+SVM is an ideal SAR image feature extraction and recognition algorithm. Although the vehicles include variations in aspect angle, target configurations and obscuration and the clutter interference is excessive, KFDA-IMED+SVM does not need image preprocessing and image segmentation and can lead to a higher recognition rate than conventional methods. Fourth, the detection and recognition are achieved by the same criterion. In addition, collecting background clutter samples in the recognition part can help reduce the false alarms in the detection part. In this paper, a detailed discussion is also presented on the influence of size of image chip on the recognition rate. In general, the simplicity, innovation and the significant effect of our vehicle detection and recognition algorithm based on KFDA meets the requirements of

SAR ATR. It is concluded to be a highly efficient vehicle detection and recognition algorithm for SAR images.

Acknowledgments

This research is supported by the National Natural Science Foundation of China, No. 61071139, No. 61471019 and No. 61171122, the Aeronautical Science Foundation of China, No. 20142051022, the Foundation of ATR Key Lab, the Fundamental Research Funds for the Central Universities, “New Star in Blue Sky” Program Foundation of Beihang University, the Royal Society of Edinburgh (RSE), and The National Natural Science Foundation of China (NNSFC) under the RSE-NNSFC joint project (2012-2014) [grant number 61211130210] with Beihang University. This research is also funded, in part, by the RSE-NNSFC joint project (2012-2014) [grant number 61211130309] with Anhui University, China; and the “Sino-UK Higher Education Research Partnership for PhD Studies” joint-project (2013-2015) funded by the British Council China and The China Scholarship Council (CSC).

References

1. Novak, L.M., M.C. Burl, and W.W. Irving. Optimal polarimetric processing for enhanced target detection. *IEEE Trans. on Aerospace and Electronic Systems*, 1993, 29(1): 234-244.
2. Wang, D. Knowledge based object detection using SAR images. *IEEE*

- International Conference on ICASSP '87, in Acoustics, Speech, and Signal Processing*, 1987.
3. Blacknell, D.. Contextual information in SAR target detection. *IEE Proc. of Radar, Sonar and Navigation*, 2001, 148(1): 41-47.
 4. Irving, W.W., L.M. Novak, and A.S. Willsky. A multiresolution approach to discrimination in SAR imagery. *IEEE Trans. on Aerospace and Electronic Systems*, 1997, 33(4): 1157-1169.
 5. Lombardo, P., M. Sciotti, and L.M. Kaplan. SAR prescreening using both target and shadow information. *Proc. of the IEEE Radar Conference*, 2001.
 6. Liu, S. and Z. Cao. SAR image target detection in complex environments based on improved visual attention algorithm. *EURASIP Journal on Wireless Communications and Networking*, 2014(1): 1-8.
 7. Bhanu, B.. Automatic Target Recognition: State of the Art Survey. *IEEE Trans. on Aerospace and Electronic Systems*, 1986, AES-22(4): 364-379.
 8. Bhanu, B. and T.L. Jones. Image understanding research for automatic target recognition. *IEEE Aerospace and Electronic Systems Magazine*, 1993, 8(10): 15-23.
 9. Bhanu, B., et al.. Guest Editorial Introduction To The Special Issue On Automatic Target Detection And Recognition. *IEEE Trans. on Image Processing*, 1997, 6(1): 1-6.
 10. Ross, T.D., et al. Standard SAR ATR evaluation experiments using the MSTAR public release data set. *International Society for Optics and Photonics in Aerospace/Defense Sensing and Controls*, 1998.
 11. Hurst, M. and R. Mittra. Scattering center analysis via Prony's method. *IEEE Trans. on Antennas and Propagation*, 1987, 35(8): 986-988.
 12. Potter, L.C. and R.L. Moses. Attributed scattering centers for SAR ATR. *IEEE Trans. on Image Processing*, 1997, 6(1): 79-91.
 13. Ross, T.D., et al. SAR ATR: so what's the problem? *An MSTAR perspective*, 1999.
 14. Lin, Y. and B. Bhanu. Evolutionary feature synthesis for object recognition. *IEEE Trans. on Systems, Man, and Cybernetics, Part C: Applications and Reviews*, 2005, 35(2): 156-171.
 15. XiaoGuang, L., H. Ping, and W. Renbiao. Two-dimensional PCA for SAR automatic target recognition. *1st Asian and Pacific Conference in Synthetic Aperture Radar*, 2007.
 16. Han, P., et al.. SAR automatic target recognition based on KPCA criterion. *Journal of electronics and information technology*, 2003, 25(10): 1297-1301.
 17. Seung, H.S. and D.D. Lee. The manifold ways of perception. *Science*, 2000, 290(5500): 2268-2269.
 18. Bryant, M.L. and F.D. Garber. SVM classifier applied to the MSTAR public data set. *International Society for Optics and Photonics in AeroSense'99*, 1999.
 19. Qun, Z. and J.C. Principe. *Support vector machines for SAR automatic target recognition*. *IEEE Trans. on Aerospace and Electronic Systems*, 2001, 37(2): 643-654.
 20. Sun, Y., et al. Synthetic aperture radar automatic target recognition using adaptive boosting. *International Society for Optics and Photonics in Defense and Security*, 2005.
 21. Dacheng, T., et al.. Geometric Mean for Subspace Selection. *IEEE Trans. on*

- Pattern Analysis and Machine Intelligence*, 2009, 31(2): 260-274.
22. Camps-Valls, G. and L. Bruzzone. Kernel methods for remote sensing data analysis. *Wiley Online Library*, 2009: Vol. 26.
 23. Vapnik, V.. *The nature of statistical learning theory*. New York: Springer, 2000.
 24. Liwei, W., Z. Yan, and F. Jufu. On the Euclidean distance of images. *IEEE Trans. on Pattern Analysis and Machine Intelligence*, 2005, 27(8): 1334-1339.
 25. Brewer, J.. Kronecker products and matrix calculus in system theory. *IEEE Trans. on Circuits and Systems*, 1978, 25(9): 772-781.
 26. Liping Hu. *Investigation on Target Recognition from SAR Images*. XiAn, China: Xidian University, 2009.
 27. Amoon, M. and G.A. Rezai-rad. Automatic target recognition of synthetic aperture radar (SAR) images based on optimal selection of Zernike moments features. *IET Computer Vision*, 2014, 8(2): 77-85.
 28. Srinivas, U., V. Monga, and R.G. Raj. SAR Automatic Target Recognition Using Discriminative Graphical Models. *IEEE Trans. on Aerospace and Electronic Systems*, 2014, 50(1): 591-606.
 29. Douville, P.L.. Measured and predicted synthetic aperture radar target comparison. *IEEE Trans. on Aerospace and Electronic Systems*, 2002, 38(1): 25-37.

Biographies



Fei Gao was born in 1975. He received his Ph.D. degree in signals and information

processing from Beihang University in 2005. He is currently an associate professor in School of Electronic and Information Engineering, Beihang University. His research interests include radar signal processing, image processing, moving target detection, etc. (E-mail: feigao2000@163.com)



Jingyuan Mei was born in 1990. He received his B.E. degree in Information Engineering School from Communication University of China. He is currently a master in School of Electronics and

Information Engineering, Beihang University. His research interests include radar signal processing, image processing, target detection, target recognition, online learning, etc.

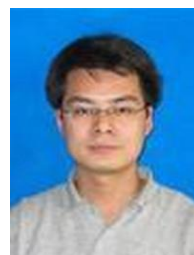
(E-mail: 347068642@qq.com)



Jinping Sun was born in 1975. He received his Ph.D. degree in signals and information processing from Beihang University in 2001. He is currently a professor of School of Electronic and

Information Engineering of Beihang University. His research interests include high resolution and advance mode SAR signal processing, image understanding and pattern recognize.

(E-mail: sunjinpingsun@buaa.edu.cn)



JunWang was born in 1972. He received his Ph.D. degree in signals and information processing from Beihang University in 2001. He is currently a Professor in school of EIE, Beihang University. His research interests include signal processing,

research interests

DSP/FPGA real-time architecture, target recognition and tracking, etc.

(E-mail: wangj203@buaa.edu.cn)



Erfu Yang received the B.E., M.E., and Ph.D. degrees from Beihang University in 1994, 1996, and 1999, respectively. He is currently a lecturer post in University of Strathclyde.

His research interests include signal processing and cognitive signal-image.

(E-mail: erfu.yang@strath.ac.uk)



Amir Hussain obtained his B.Eng. (with 1st Class Honors) and Ph.D., both in electronic and electrical engineering from the University of Strathclyde in Glasgow, Scotland, in 1992 and 1996, respectively. He is

currently a Professor in School of Natural Sciences, University of Stirling and founding Director of the Cognitive Signal-Image and Control Processing Research (COSIPRA) Laboratory. His research interests are mainly interdisciplinary, and include machine learning and cognitive computing for modeling and control of complex systems.

(E-mail: kfa@cs.stir.ac.uk)

第一作者姓名: 高飞

主要研究方向: 雷达信号处理、图像处理、目标检测系统、目标跟踪与识别

职称: 副教授 学历: 博士

手机: 13681444428 固话: 01082317240

E-mail: feigao2000@163.com

地址: 北航 203 教研室 邮编: 100191

第二作者姓名: 梅净缘

主要研究方向: 雷达信号处理、图像处理、目标检测与识别、在线学习

职称: 无 学历: 硕士

手机: 13581861319 固话: 01082317240

E-mail: 347068642@qq.com

地址: 北航 203 教研室 邮编: 100191

第三作者姓名: 孙进平

主要研究方向: 信号处理、图像感知、模式识别

职称: 教授 学历: 博士

手机: 13501097201 固话: 01082317240

E-mail: sunjinping@buaa.edu.cn

地址: 北航 203 教研室 邮编: 100191

第四作者姓名: 王俊

主要研究方向: 信号处理、DSP/FPGA 实时

职称: 教授 学历: 博士

手机: 13541831972 固话: 01082319474

E-mail: wangj203@buaa.edu.cn

地址: 北航 203 教研室 邮编: 100191

第五作者姓名: 杨尔辅

主要研究方向: 信号处理、图像认知

职称: 教授 学历: 博士

手机: 固话: +44 (0) 141 548 2919/4294

E-mail: erfu.yang@strath.ac.uk

地址: 斯克莱德大学 邮编: Glasgow G1 1XJ, UK

第六作者姓名: Amir Hussain

主要研究方向: 信号处理、图像认知

职称: 教授 学历: 博士

手机: 固话: +441786467421

E-mail: kfa@cs.stir.ac.uk

地址: 斯特林大学 邮编: Stirling FK9 4LA